Journal of Research and Applications in Mechanical Engineering
ISSN: 2229-2152 (Print); 2697-424x (Online)
(2023) Vol. 11, No. 2, Paper No. JRAME-23-11-013
[DOI: 10.14456/jrame.2023.13]

Research Article

Numerical Investigation for Aerodynamic Noise of a Low Mach Number Axial Fan

A. Ketpunya[1,2]
C. Chumchan[1,3]
N. Moonpa[4]
K. Tontiwattanakul[1,2,*]
[1] *Sound and Vibration Research Group, King Mongkut's University of Technology North Bangkok, Bangkok 10800, Thailand*
[2] *Department of Mechanical and Aerospace Engineering, Faculty of Engineering, King Mongkut's University of Technology North Bangkok, Bangkok 10800, Thailand*
[3] *Department of Power Engineering Technology, College of Industrial Technology, King Mongkut's University of Technology North Bangkok, Bangkok 10800, Thailand*
[4] *Mechanics, Materials, and Engineering Design Research Group, MMED, Rajamangala University of Technology Lanna, Chiangmai 50300, Thailand*

Received 23 January 2023
Revised 19 April 2023
Accepted 8 May 2023

Abstract:
Typically, the noise generated by axial fans arises from both the motion of mechanical parts and the turbulence of the airflow. When the airflow interacts with the stationary and rotating surfaces of an axial fan, aerodynamic noise is produced. To investigate this phenomenon, the study used unsteady Computational Fluid Dynamics (CFD) simulations with Large Eddy Simulation (LES) to capture the turbulent flow field. The Direct Simulation Method (DSM) and Ffowcs Williams & Hawkings (FW-H) method were used to predict the Sound Pressure Level (SPL) spectra of the aerodynamic noise. The results show that the SPL spectra trend from the DSM and FW-H is consistent at various receive points. However, the SPL spectra from the DSM are lower than that from the FW-H in the far-field noise region. Moreover, the main noise source of an axial fan is found on the propeller surface, which is dominated at the leading edge near the blade tip region.

Keywords: *Direct simulation method, Ffowcs Williams and Hawkings, Aerodynamic noise, Axial fan noise*

1. Introduction

Fans are widely used in both industrial and residential settings, with applications ranging from small electronic components to large building ventilation systems. However, the issue of environmental noise has become increasingly important in social development due to its negative impact on human health and well-being. Exposure to high levels of noise pollution can lead to physical and psychological health problems, such as hearing loss, cardiovascular disease, and stress [1, 2]. Consequently, techniques for improving fan noise have become a focal point of investigation for many researchers [3-5].

The noise produced by fans is caused by mechanical components and aerodynamic noise. The most common and identifiable aerodynamic noise emitted from the fan can be classified into tonal noise and broadband noise. Tonal noise is generated by the airflow across the blade and the aerodynamic force exerted on the fluid by the blade surface and blade-vortex interaction [6]. The Blade Passing Frequency (BPF) has a high acoustic amplitude, which is the main tonal noise [7].

* Corresponding author: K. Tontiwattanakul
E-mail address: khemapat.t@eng.kmutnb.ac.th

On the other hand, broadband noise results from turbulent flow over the blade, which is a random and non-periodic signal. From the previous study, Tip Leakage Flow (TLF) and Tip Leakage Vortex (TLV) between the blade tip and shroud are the main dominant broadband noise source [8]. Moreover, the TLV has adverse impacts on fan performance, including airflow rate [9] and energy loss [10].

The Reynolds Averaged Navier Stokes (RANS) equation with turbulence modelling and LES are commonly used for estimating the flow field [11]. RANS is conducted for steady flow simulation, and its results are used as initial conditions in unsteady state simulation. On the other hand, LES is applied for unsteady state simulation to capture pressure fluctuations around the blade and shroud. Afterwards, the DSM and FW-H are used to predict the noise generated by the airflow. In a previous study, Hodor et al. [12] used the LES model combined with FW-H to predict aerodynamic noise. Gloerfelt X et al. [13] used DSM to predict the noise generated from airflow through a rectangular strait and then compared it with experimental results and prediction results from FW-H.

The simulation results from both methods appear to be consistent with the measurements and provide reasonably accurate predictions. However, both methods have their own advantages and limitations when applied to different problems. Despite this, there is a lack of previous research comparing the performance of these two methods in the context of an axial fan. The unsteady CFD simulation is computed from LES; to capture the turbulence flow field. Afterwards, DSM and FW-H are applied to predict the SPL spectra characteristic of the aerodynamic noise. This study aims to identify the strengths and limitations of each approach in predicting aerodynamic noise generated by axial fans. This study also aims to compare the SPL spectra characteristics of DM and FW-H method and the main noise source. Such a study would contribute to the advancement of knowledge in the field of fan simulation and modeling, ultimately helping to determine the most suitable method for axial fan aeroacoustics simulation.

2. Numerical Simulation

2.1 3D Modelling

In this work, the geometry of the axial fan for the present study is shown in Fig. 1. The fan geometry consists of two parts, a propeller and a shroud. The NACA 4-digit airfoil series was used in this work. The main parameters of the fan's geometry are shown in Table 1. The three-dimensional geometry is created by SolidWorks software. ANSYS SpaceClaim is used to design a computational domain, which is divided into rotating and stationary parts. The rotating domain has represented the air in the region near a propeller. On the other hand, the stationary domain has demonstrated the air that encloses the fan. However, both the inlet and outlet are extended enough to capture a fluid flow and noise behaviour, which is required for DSM. The dimensions of two domains and the boundary condition are shown in Fig. 2.

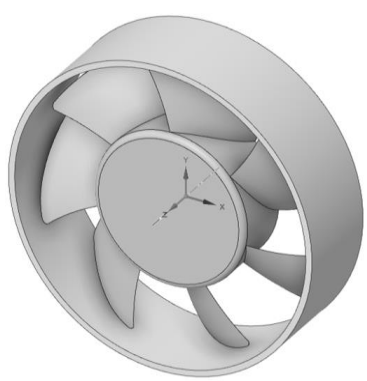

Fig. 1. Fan geometry.

Table 1: Main parameters of the fan geometry.

Parameter	Value
Number of blades	7
Max. rotor speed	7500 rpm
Shroud diameter	121 mm
Hub diameter	63 mm
Blade tip chord	42 mm
Blade tip radius	57.5 mm
Tip-clearance	3.15 mm
Blade tip speed	45.16 m/s

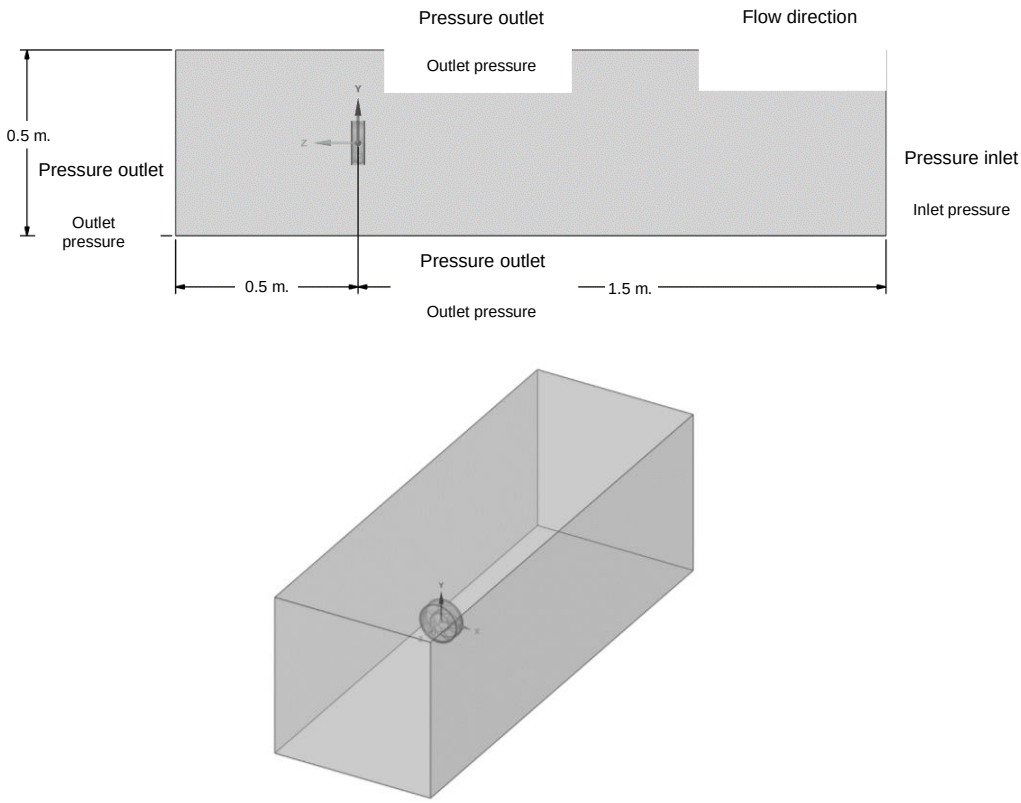

Fig. 2. Computational domain.

2.2 Mesh Generation

ANSYS Fluent meshing was used for mesh generation in this work. The mesh was created using poly-hexcore technology, which reduces computational time and the number of elements while increasing accuracy [14]. The computational domains consist mainly of structured hexahedral elements, with complex zones being filled with unstructured polyhedral elements. The boundary layer at the shroud is filled with poly-prism elements consisting of five layers. The region around the fan is subsequently refined to increase the resolution of the unsteady flow field in the vicinity of the fan. A mesh independence study was conducted using steady simulation, gradually increasing the number of elements in a computational domain until the inlet velocity converges to a constant value, as shown in Fig. 3. Therefore, 1.3 million elements were used for this simulation. The details of mesh generation are shown in Fig. 4.

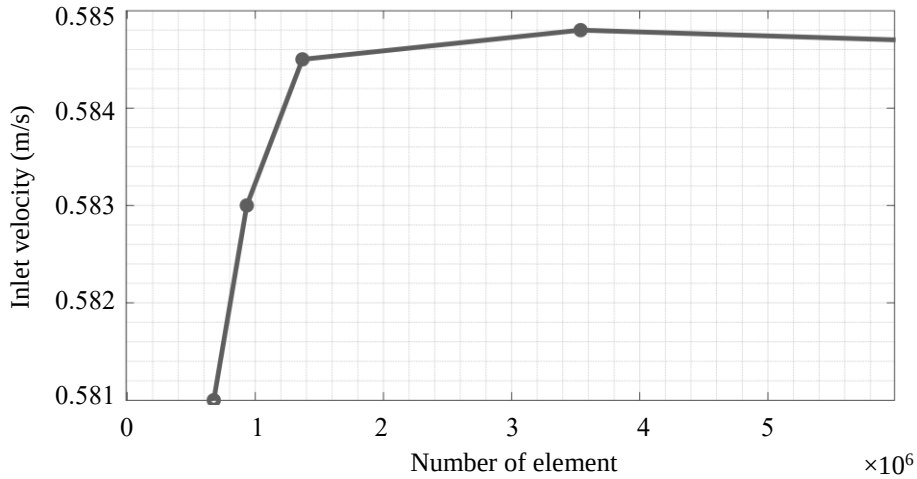

Fig. 3. Mesh independent study.

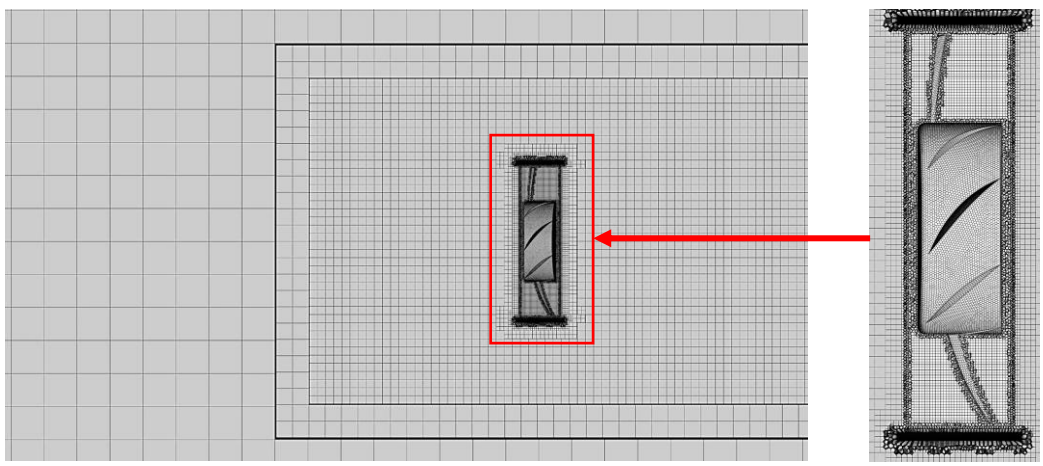

Fig. 4. Poly-hexcore mesh with 1.3 million elements number.

2.3 Numerical Method

The numerical model consisted of the flow field and aeroacoustics. For the flow field prediction, the standard k-ε turbulence model is Reynolds time averaging and one of the most popular models for a steady flow, which describe the phenomena of turbulence flow. However, the Renormalization Group (RNG) k-ε model has used a renormalization group mathematical method to renormalize the Navier-Stokes equations. It is similar in form to the standard k-ε model, which improves the accuracy of turbulence flow prediction. On the other hand, LES is a volume averaging, which reduces complexity by focusing on turbulence larger length scales as well as larger time scales. LES is the most popular model for an unsteady flow and aeroacoustics estimation. The Mach number is a dimensionless quantity that represents the ratio of the speed of an object or fluid to the speed of sound in the surrounding medium. The Mach number is calculated by

$$Ma = \frac{v}{c_0} \tag{1}$$

where v is the velocity of the object or fluid and c_0 is the speed of sound. The Mach number is divided into various ranges, each indicative of different types of flow behavior, including subsonic ($Ma < 1$), transonic ($Ma \approx 1$), supersonic ($Ma < 1$), and hypersonic ($Ma < 5$) flows.

In the context of this study, the Mach number has been determined to be 0.133 based on the calculation using the blade tip speed of 45.16 m/s. This indicates that the fan is operating in a subsonic flow or at a low Mach number. For the aeroacoustic prediction, DSM is based on the direct computation of the fluid dynamics equation, such as URAN and LES [11]. To predict noise using DSM, static pressure is used to compute the acoustic pressure, which represents the fluctuations resulting from sound waves propagating through the fluid. In contrast, the integral method by FW-H is based on Lighthill's acoustic analogy [15, 16]. The FW-H method [17] is used to predict the pressure fluctuation source on the moving surface. The FW-H equation can be written as:

$$\frac{1}{c_0^2}\frac{\partial^2 p'}{\partial t^2} - \nabla^2 p' = \frac{\partial^2}{\partial x_i \partial x_j}\left\{T_{ij} H(f)\right\} - \frac{\partial}{\partial x_i}\left\{\left[P_{ij} n_j + \rho u_i (u_n - v_n)\right]\delta(f)\right\} + \frac{\partial}{\partial t}\left\{\left[\rho_0 v_j + \rho(u_n - v_n)\right]\delta(f)\right\} \quad (2)$$

where ρ' is acoustic pressure at the far field, ρ is fluid density, ρ_0 is free stream fluid density, P_{ij} is the compressive stress tensor, n_j is the surface unit normal vector, u_i is fluid velocity component in the x_i direction, u_n is fluid velocity component normal to the surface, v_n is surface velocity component normal to the surface, $\delta(f)$ is Dirac delta function, $H(f)$ is Heaviside function, and T_{ij} is the Lighthill stress tensor.

In Equation 2, the left-hand side represents pressure wave propagation, while the three terms on the right side (from left to right) represent the quadrupole, dipole, and monopole respectively. For a low Mach number condition, the radiation from the quadrupole source is small compared to that from monopole and dipole sources. Therefore, the quadrupole source can usually be neglected [11].

2.4 Numerical Setup for Flow Field and Aeroacoustics Prediction

ANSYS Fluent was used to simulate both the flow field and aeroacoustics. The three-dimensional CFD simulation setup consisted of steady and unsteady simulations with pressure-based and incompressible flow assumptions. The k-ε turbulence model with RNG was selected for the steady simulation. A reference frame motion of 7,500 rpm was applied for the rotating domain. The results of the steady simulation were used as the initial values in the unsteady simulation, which utilized the LES with the Smagorinsky-Lilly model. Furthermore, the FW-H equation was enabled for the unsteady simulation. The mesh motion with the same rotational speed as the steady case was conducted for the rotating domain, and the time step size was defined by the frequency bandwidth at 5,000 Hz. The steady and unsteady simulations had the same setup, with both boundary conditions being inlet pressure and outlet pressure with an atmospheric pressure of 101,325 Pascal. The SIMPLEC algorithm was used as the simulation method with the second order of pressure, momentum, turbulent kinetic energy, and turbulent dissipation ratio.

3. Results and Discussion

3.1 Comparison between DSM and FW-H

Figure 5 illustrates a contrast of the SPL frequency spectra between DSM and FW-H at various receiving locations. Receiving points were established at four different locations relative to the fan inlet: 0.15 m, 0.2 m, 0.6 m, and 1 m. The predicted SPL spectra from DSM exhibit a similar frequency trend to that of FW-H across the entire frequency range of interest, as depicted in Figures 5a and 5b. Figures 5c and 5d show a decrease in SPL spectra for both methods, which can be attributed to the inverse square law relationship between sound intensity and distance. Under far-field conditions, the SPL spectra from DSM decreased more significantly than that from FW-H, leading to a discernible difference in the SPL spectra results between the two methods. DSM can capture pressure fluctuations in the turbulence field but may not fully account for the propagation of acoustic waves. This can result in differences in the results obtained at varying distances from the noise source in far-field conditions. On the other hand, the FW-H method captures acoustic wave propagation from pressure fluctuations on the source surfaces, excluding the turbulent field. Consequently, the predictions obtained from FW-H are accurate for aeroacoustics at various distances. Moreover, The DSM requires a large simulation domain that extends over the acoustics receiving point and the flow region, but FW-H does not necessarily require such a large domain. Hence, the DSM incurs a higher computational cost than FW-H.

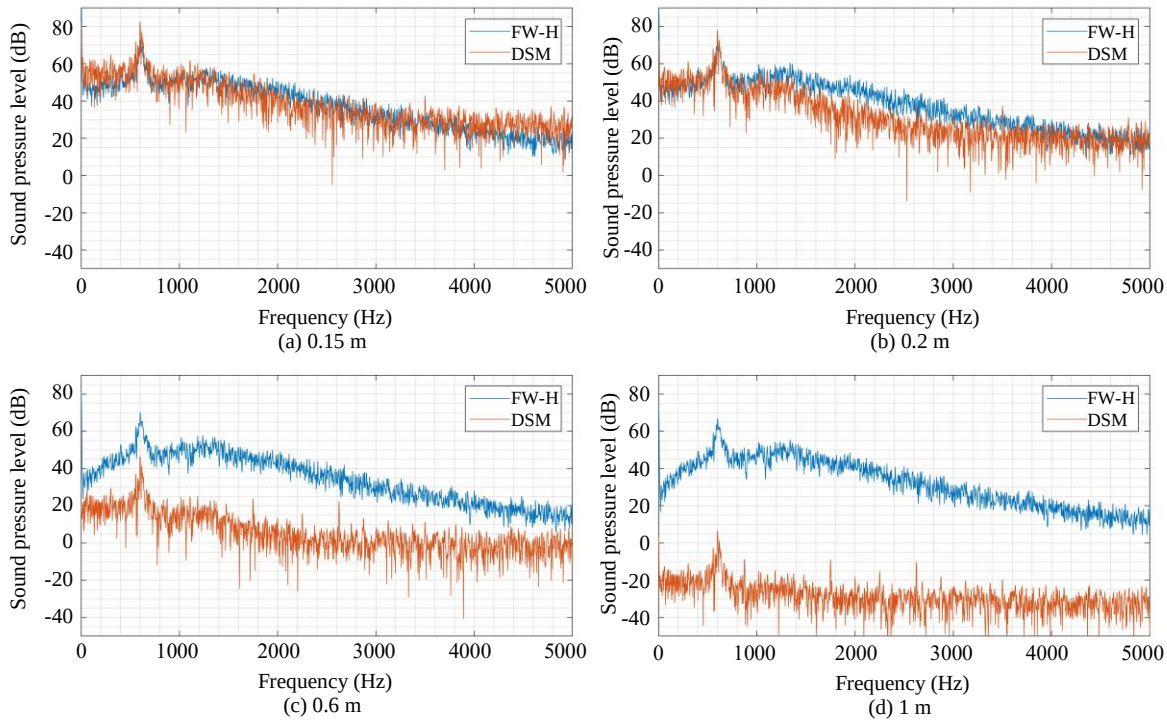

Fig. 5. SPL spectra.

3.2 Discussion of Fan Noise

This section presents a comparison of the BPF at two different rotor speeds and discusses the main noise source of an axial fan. Figure 6 shows the pressure fluctuation spectra at the BPF. The results indicate that the BPF occurred at 586 Hz when the blades rotated at 7,500 rpm. This investigation produced inconsistent results with the analytical solution, which predicted that the BPF should appear at 875 Hz. To validate the predicted results, an additional study was conducted to examine the BPF at 4,500 rpm. The results of this study show that the BPF occurred at 348 Hz, which is also inconsistent with the analytical solution. However, the ratio between the predicted and analytical results is the same for both studies, with a ratio of 0.66.

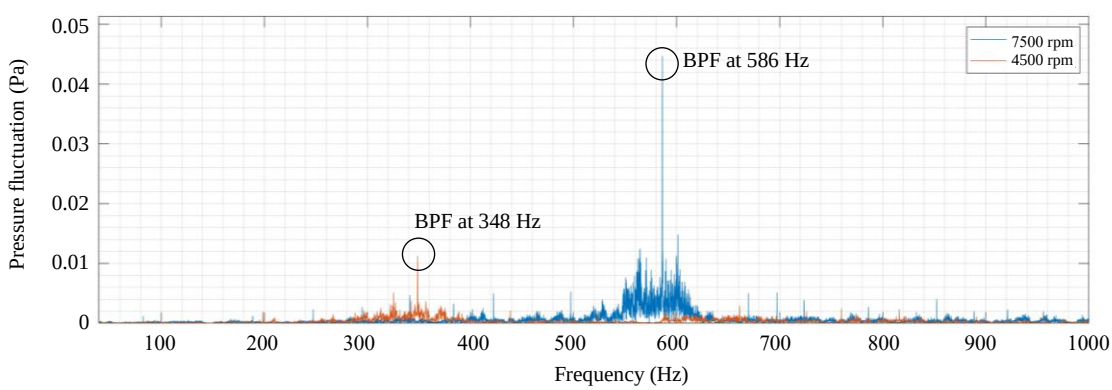

Fig. 6. Pressure fluctuations spectra.

The pressure time derivative represents the strength of the acoustic source. Figure 7 presents the power spectral of the pressure time derivative contour on the blades and shroud surfaces at a dominant frequency band of 630 Hz in a 1/3 octave frequency spectral. This contour was calculated using data from FW-H at the flow time between 0.3 to 0.55 s. The results show that the power spectral of the pressure time derivative on the leading edge near the blade tips is higher than in other areas.

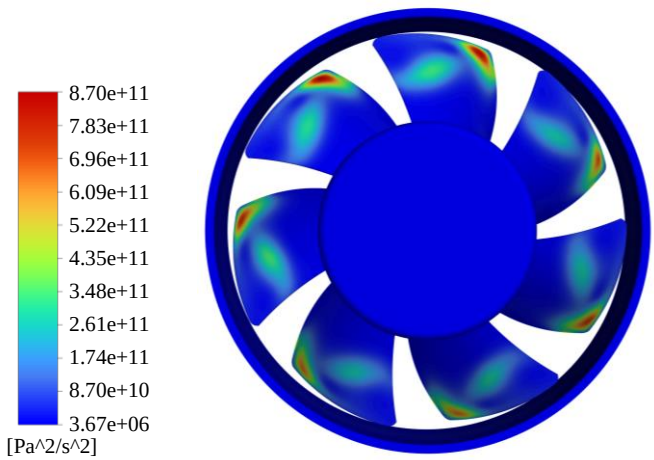

Fig. 7. The power spectral of pressure time derivative contour at 630 Hz.

4. Conclusion

This paper presents the creation and simulation of an axial fan model to investigate two simulation methods for noise prediction, specifically DNS and FW-H. The results from FW-H are used to examine an inconsistent BPF and locate the main noise source. The conclusions of the study are summarized as follows:

1. The near-field SPL spectra predicted by DSM and FW-H exhibit a similar frequency trend across the entire frequency range of interest, but the SPL spectra from DSM decrease more significantly than that from FW-H under far-field conditions due to its inability to fully account for the propagation of acoustic waves. FW-H method captures acoustic wave propagation from pressure fluctuations on the source surfaces, excluding the turbulent field, making its predictions accurate for aeroacoustics at various distances. Moreover, DSM requires a larger simulation domain, leading to a higher computational cost than FW-H. In summary, both the DSM and FW-H methods have their own advantages and disadvantages, and the decision on which to use will depend on the specific requirements of the application. DSM is suitable for predicting near-field regions, while FW-H method is suitable for far-field regions.

2. The BPF obtained from the prediction and analytical solutions is inconsistent, with a constant ratio of 0.66 between the predicted and analytical values. This constant ratio will be verified in future research. Furthermore, the main noise source of an axial fan was found to be located on the propeller, specifically at the leading edge near the blade tip. In future research, the author will compare prediction results with experimental data and investigate the factors that contribute to the leading-edge noise.

Nomenclature

Ma	Mach number
v	velocity of the object or fluid, m/s
c_0	Speed of sound, m/s
p'	Acoustic pressure, Pa
ρ	Fluid density, kg/m^3
ρ_0	Free stream fluid density, kg/m^3
P_{ij}	Compressive stress tensor, Pa
n_j	Surface unit normal vector

x_i Direction
u_i Fluid velocity component the x_i direction, m/s
u_n Fluid velocity component normal to the surface, m/s
v_n Surface velocity component normal to the surface, m/s
$\delta(f)$ Dirac delta function
$H(f)$ Heaviside function
T_{ij} Lighthill stress tensor, Pa

Subscripts
CFD computational fluid dynamics
LES large eddy simulation
DSM direct simulation method
FW-H Ffowcs Williams & Hawkings
BPF blade passing frequency
TLF tip leakage flow
TLV tip leakage vortex
RANS Reynolds Averaged Navier Stokes

Acknowledgement

The authors would like to thank Mr. Thoranin Oonariya and Mr. Jiraphan Inthian from iRAP robot community; for accommodating in 3D modelling procedure. This research is supported by the Research Project of Tripartite Education System Using Work Based Learning.

References

[1] Münzel T, Gori T, Babisch W, Basner M. Cardiovascular effects of environmental noise exposure. Eur Heart J. 2014;35(13):829-836.
[2] Pinosova M, Andrejiova M, Badida M, Moravec M. Analysis and evaluation of risks from exposure to noise in a working environment. Acta Mechanica Slovaca. 2018;22(3):44-52.
[3] Wu L, Liu X, Wang M. Effects of bionic volute tongue on aerodynamic performance and noise characteristics of centrifugal fan used in the air-conditioner. J Bionic Eng. 2020;17(4):780-792.
[4] Jiang B, Wang J, Yang X, Wang W, Ding Y. Tonal noise reduction by unevenly spaced blades in a forward-curved-blades centrifugal fan. Appl Acoust. 2019;146:172-183.
[5] Killeen J, Davis I, Wang J, Bennett GJ. Fan-noise reduction of data centre telecommunications' server racks, with an acoustic metamaterial broadband, low-frequency sound-absorbing liner. Appl Acoust. 2023;203:109229.
[6] Glegg S, Devenport W. Open rotor noise. In: Aeroacoustics of Low Mach Number Flows. London: Academic press; 2017. pp. 399-436.
[7] Park M, Lee DJ, Lee H. Inflow effects on tonal noise of axial fan under system resistances. Appl Acoust. 2022;192:108737.
[8] Luo B, Chu W, Zhang H. Tip leakage flow and aeroacoustics analysis of a low-speed axial fan. Aerosp Sci Technol. 2020;98:105700.
[9] Khalid SA, Khalsa AS, Waitz IA, Tan CS, Greitzer EM, Cumpsty NA, et al. Endwall Blockage in Axial Compressors. J Turbomach. 1999;121(3):499-509.
[10] Denton JD. The 1993 IGTI Scholar Lecture: Loss Mechanisms in Turbomachines. J Turbomach. 1993;115(4):621-656.
[11] Ansys. Ansys fluent theory guide [Internet]. 2022 [cited 2022]. Available from: http://www.ansys.com.
[12] Hodor V, Birle D, Nascutiu L, Deac I. Aeroacoustics -noise prediction by using 'LES' for signal processing. Energy Procedia. 2017;112:322-329.
[13] Gloerfelt X, Bailly C, Juvé D. Direct computation of the noise radiated by a subsonic cavity flow and application of integral methods. J Sound Vib. 2003;266(1):119-146.
[14] Zore K, Sasanapuri B, Parkhi G, Varghese A. Ansys mosaic poly-hexcore mesh for high-lift aircraft configuration. 21st Annual CFD Symposium; 2019 Aug 8-9, Bangalore. p. 1-11.

[15] Lighthill MJ. On sound generated aerodynamically I. General theory. Proc R Soc Lond A Math Phys Sci. 1952;211(1107):564-587.
[16] Lighthill MJ. On sound generated aerodynamically II. Turbulence as a source of sound. Proc R Soc Lond A Math Phys Sci. 1954;222(1148):1-32.
[17] Ffowcs Williams JE, Hawkings DL. Sound generation by turbulence and surfaces in arbitrary motion. Philos Trans R Soc Lond A Math Phys Sci. 1969;264(1151):321-342.